# INVESTIGATION OF A SELF-ACTUATED, GRAVITY-DRIVEN SHUTDOWN SYSTEM IN A SMALL LEAD-COOLED REACTOR

**Govatsa Acharya, Fredrik Dehlin, Sara Bortot and Ignas Mickus**
KTH, Division of Nuclear Engineering,
Albanova University Center, 10691 Stockholm, Sweden

govatsa@kth.se, fdehlin@kth.se, bortot@kth.se, mickus@kth.se

## ABSTRACT

Passive safety systems in a nuclear reactor allow to simplify the overall plant design, beside improving economics and reliability, which are considered to be among the salient goals of advanced Generation IV reactors. This work focuses on investigating the application of a self-actuated, gravity-driven shutdown system in a small lead-cooled fast reactor and its dynamic response to an initiating event. The reactor thermal-hydraulics and neutronics assessment were performed in advance. According to a first-order approximation approach, the passive insertion of shutdown assembly was assumed to be influenced primarily by three forces: gravitational, buoyancy and fluid drag. A system of kinematic equations were formulated *a priori* and a MATLAB program was developed to determine the dynamics of the assembly. Identifying the delicate nature of the balance of forces, sensitivity analysis for coolant channel velocities and assembly foot densities yielded an optimal system model that resulted in successful passive shutdown. Transient safety studies, using the multi-point dynamics code BELLA, showed that the gravity-driven system acts remarkably well, even when accounting for a brief delay in self-actuation. Ultimately the reactor is brought to a sub-critical state while respecting technological constraints.

KEYWORDS: Self-actuated passive system, gravity-driven shutdown system, small modular reactor, lead-cooled fast reactor

## 1. INTRODUCTION

Safety is one of the important aspects in the design of a nuclear reactor. It has been accorded greater attention since the accidents in Chernobyl and, more recently, in Fukushima. As a part of the safety architecture a majority of the reactor designs incorporate reactor control systems and reactor shutdown systems. In order to overcome shortcomings, such as issues with reliability and operability under drastic conditions, in the drive mechanisms of active shutdown systems, passively operated shutdown systems are conceptualised. Gravity-driven or -assisted insertion is one of the preferred solutions to the question of passive safety in shutdown system. The underlying idea here is to make use of the self-weight of the absorber rods to drive the assembly without any external drive mechanism. A carefully designed gravity-driven shutdown system is reliable in diverse accident scenarios. Such passive systems have been used in water-cooled reactors, for instance in CANDU reactors, and have been tested in sodium-cooled fast reactors. This has not been the case in lead-cooled fast reactors (LFRs). Liquid lead, on account of its high density

and consequently high buoyancy, is not conducive to insertion by gravity. MYRRHA in the lead-bismuth eutectic (LBE) configuration is one reactor that, despite having a dense coolant, proposes this method of shutdown [1]. However, not much information is available regarding this passive system in the public domain. Moreover, LFRs have the potential for buoyancy-driven insertion, although this shutdown route is fraught with design challenges, requiring insertion from below the core and is not suited for small modular reactors (SMRs). To overcome buoyancy force a gravity-driven system in LFR design mandates the use of dense materials which reduces the choice of candidate materials for the absorber rods. Recent developments in super-hard ceramic borides seem very promising, both from the point of design requirements and economics. Numerical study to demonstrate the viability of implementing this concept in a small LFR is presented in this paper.

## 2. SMALL LEAD-COOLED REACTOR

LeadCold Reactors, a spin-off company of KTH Reactor Physics Division, is developing LFRs in the SMR category. Their *SwEdish Advanced LEad Reactor* (SEALER) is designed to produce electricity in remote, off-grid regions, such as the Canadian Arctic [2]. A variant of SEALER is currently being developed for the UK, named *Small, Economic and Agile LEad-cooled Reactor for the UK* (SEALER-UK). This is a 55MWe LFR fuelled with 11.8% enriched uranium nitride (UN). Uranium nitride is the choice for the fuel to achieve a critical core in compact design with enhanced fuel performance and utilization. The design proposes austenitic grade 1515Ti(Si) steel, coated with a layer of alumina forming Fe10Cr6Al-RE [3], as the clad material. The reactor core has 85 hexagonal fuel assemblies surrounded by 6 control assemblies comprising boron carbide ($B_4C$) rods, with natural boron. Additionally, for safe-shutdown of the reactor, 6 shutdown assemblies are present at the periphery of the core. The shutdown rods are proposed to be made of tungsten-rhenium diboride ($WReB_2$), while the reflectors are of yttrium-stabilised zirconia (YSZ). The coolant inlet and outlet temperatures are 420$^o$C and 550$^o$C respectively.

### 2.1. Thermal-hydraulics and Neutronics Description

The steady state thermal-hydraulics calculations were performed for the hottest channel in the core using a simplified 1D model to evaluate temperature profiles of the fuel and coolant. The heat flux profile of the fuel pellet was assumed to be cosinus and transmitted to the coolant radially. Appropriate correlations for thermo-physical properties of fuel, clad and coolant were used. In particular, Hayes' correlation for UN [4] and Banerjee's correlation for 1515Ti(Si) steel [5] were used. Mikityuk's correlation [6] for convective heat transfer coefficient was used for the triangular lattice in fuel bundle. The results from this model in the active zone (AZ) are presented in Fig. 1a.

The hot-state model of the core was implemented in the Monte-Carlo codes Serpent [7] and OpenMC [8], after ascertaining the hot dimensions assuming thermal expansion from cold dimensions. In the Serpent burnup calculations the point of maximum uncontrolled reactivity was determined as the critical point, occurring 17.5y after startup and the kinetic parameters were extracted at this critical point. Reactivity coefficients and the reactivity worth of shutdown rods were calculated independently in Serpent and OpenMC. Plot of the reactivity worth of the shutdown rod against its length, known as the *S-Curve* as presented in Fig. 1b, was evaluated by inserting the shutdown bank into the reactor in steps from the parking position (U), along the upper lead plenum, the AZ and the lower lead plenum, to the bottom (L) of the core.

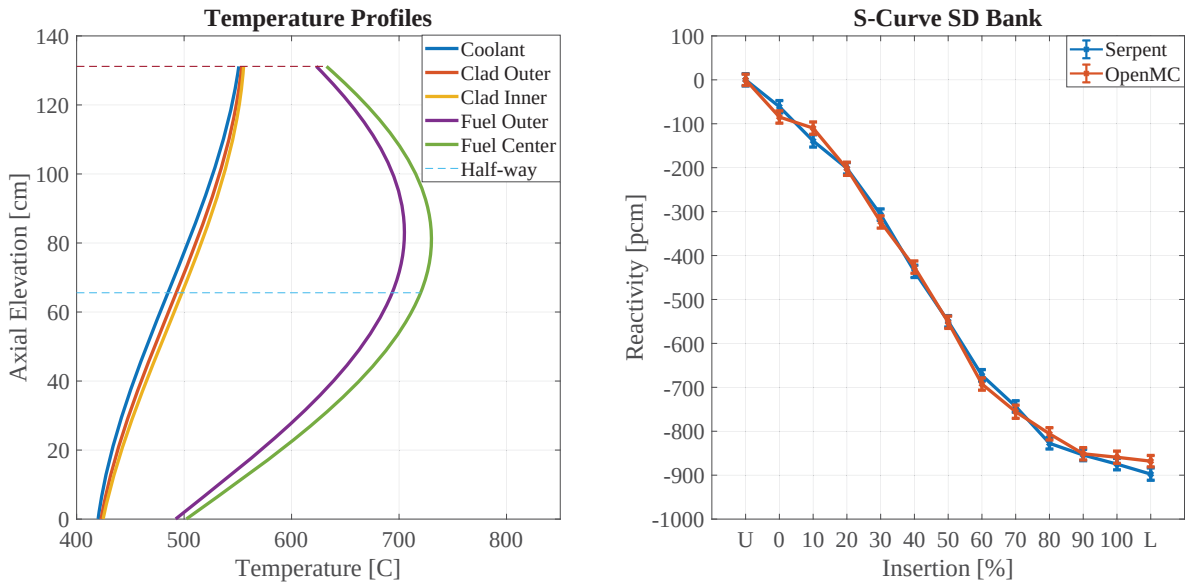


**(a) Temperature Profiles of the Fuel, Clad and Coolant** **(b) *S-Curve* of the Shutdown (SD) Assembly Bank**

**Figure 1: Thermal-hydraulics and Neutronics Results**

## 3. SHUTDOWN SYSTEM

For a material to *sink* in liquid lead it should theoretically be denser than 10.7g/cm$^3$, the melting density of lead. The recently developed tungsten-rhenium diboride solid-solution [9] is a promising material that satisfies this condition. This ceramic is formed by dissolving tungsten diboride ($WB_2$) in rhenium diboride ($ReB_2$). The density of the solid-solution decreases with increasing tungsten fraction as a result of changing crystallographic structure. Keeping in mind the economics of these exotic materials, the tungsten fraction was assumed to be 48% atomic, the limit of solubility of $WB_2$ in the solution. Having this high tungsten fraction will minimise the overall cost as the price of rhenium (2,800$/kg [10]) is roughly 93 times that of tungsten (30$/kg [11]). The theoretical density at this atomic fractions is 12.3g/cm$^3$ which at a manufacturing porosity of 5% yields 11.7g/cm$^3$. This material has been shown to be an effective neutron absorber [12] and is therefore an excellent material satisfying the requirements for passive insertion.

### 3.1. System Model Description

Each shutdown assembly comprises 7 absorber rods that have Fe10Cr4Al clad encasing the absorber pellets. A wrapper made of the same steel houses the absorber rod bundle. Precise description of the assembly was minimal in the current engineering design and some simplifications were made in the model. The assembly model was assumed to be composed of the rod bundle with the wrapper and an assembly foot. As a first-order approximation the motion of the assembly, as it falls due to gravity, is described by the following forces: *gravitational force* acting downwards, *buoyancy force* acting upwards and *fluid drag force* acting against the motion. The net force acting can be expressed as $F_{net} = F_{gravitational} - F_{buoyancy} - F_{drag}$. Here, $F_{gravitational}$ is the total force of the individual components (pellet, clad, foot) due to gravity, computed as $\Sigma m_{component} \cdot g$,

$F_{buoyancy}$ is the total force of the submerged volume of the assembly components (pellet, gas gap, clad, foot), computed as $\Sigma v_{displaced} \cdot \rho_{pb} \cdot g$ and $F_{drag}$ is the force due to fluidic resistance to motion. The coolant in the channel was divided into three regions corresponding to the upper lead plenum (constant temperature of 550$^o$C), the AZ (varying temperature according to Fig. 1a) and the lower lead plenum (constant temperature of 420$^o$C), shown representatively in Fig. 2.

Unlike the other forces, computing drag force is more cumbersome as it is a combination of forces and to keep the calculations simple, pressure drag and skin-friction drag were considered in the model, i.e. $F_{drag} = F_{pressure} + F_{skin-friction}$. Pressure drag is due to resistive forces exerted parallel to flow direction while skin-friction drag arises from shear forces along the object's surface. As the assembly is inserted, lead flows relative to the assembly and it was assumed here that the pressure component acts on the profile or form of the assembly foot, while the skin-friction component acts only along the outer walls of the wrapper. A general expression for the two drag forces is $F_{drag} = \frac{1}{2} A \cdot \rho_{pb} \cdot v_{rel}^2 \cdot C$. Here, $A$ is the area: wall surface area for the skin-friction component and foot cross-section area for the pressure component, $v_{rel}$ is the relative velocity, i.e. $v_{assembly} + v_{coolant}$, between the assembly and the coolant, and $C$ is the drag coefficient.

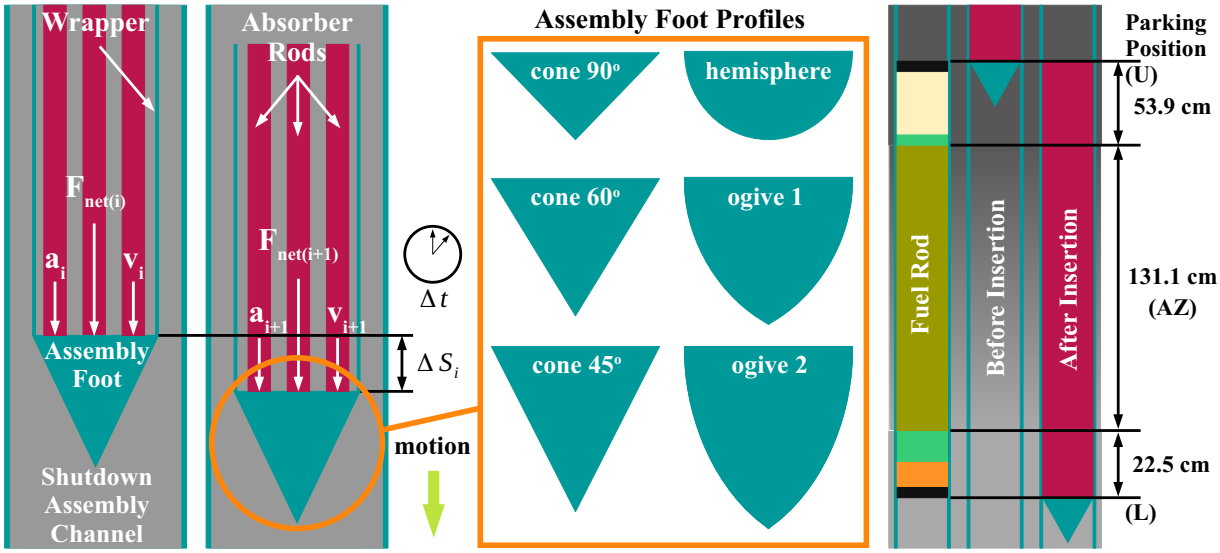


**Figure 2: Representative Images of the Assembly Insertion Model, Idealised 2D Sections of the Assembly Foot and the Different Regions Considered in the Channel**

Skin-friction coefficient was computed considering mixed laminar-turbulent flow over a flat plate given as $C = \frac{0.074}{Re_L^{0.2}} - \frac{1742}{Re_L}$, where $Re_L$ is the Reynolds number, whereas pressure coefficient is dependent on the profile of the assembly foot. Preliminary calculations showed this coefficient is very crucial for passive insertion. On account of lack of detailed designs of the foot, simplified profiles were considered, as shown in Fig. 2, in the CFD simulations that were run using ANSYS Fluent. Drag coefficients were determined for different $Re$, as it is not constant and depends on flow characteristics. The flat profile was found to have the highest drag and 45$^o$ cone profile the least drag. An exponential function fit for the variation of drag coefficient with velocity, ranging from 0.05m/s to 2m/s, of the 45$^o$ cone profile was used in the final expression of the pressure drag force. The coolant inside the wrapper was considered to not contribute to any drag forces as it was deemed to be relatively stationary in comparison to the coolant flowing on the outside.

### 3.2. Numerical Simulation Method

A MATLAB program was developed that solves the kinematic equations at discretised time steps for the defined system model description. Starting from an initial parking position above the core, the assembly is allowed to fall due to gravity, as shown in the idealised representation in Fig. 2, and during each time step the acceleration, the velocity, the distance travelled, the buoyancy, drag and net forces are calculated, in addition to the time taken to reach the bottom of the core.

Initial runs of the program revealed that the solid cone of the assembly foot, considered to be made of Fe10Cr4Al steel, was too voluminous that its contribution to buoyancy force exceeded its contribution to gravitational force. Fe10Cr4Al has a density of 8.25g/cm$^3$ whereas the average lead density in the channel is 10.47g/cm$^3$, implying that upward buoyancy is greater. This required adding weights to the assembly, practically in the form of tungsten (maximum theoretical density 19.00g/cm$^3$) ballast, which in the program was done by increasing the density of the foot material. Fig. 3a depicts the impact of increasing the density of the foot material on the dynamics of insertion. In addition, the coolant flow in the shutdown assembly channel was found to have an appreciable impact on account of its contribution to drag forces. Fig. 3b presents the variation of the dynamics with decreasing coolant velocity, from 0.84m/s (average coolant velocity in the outer fuel assemblies) to 0m/s (practically there would be non-zero velocity due to free convection).

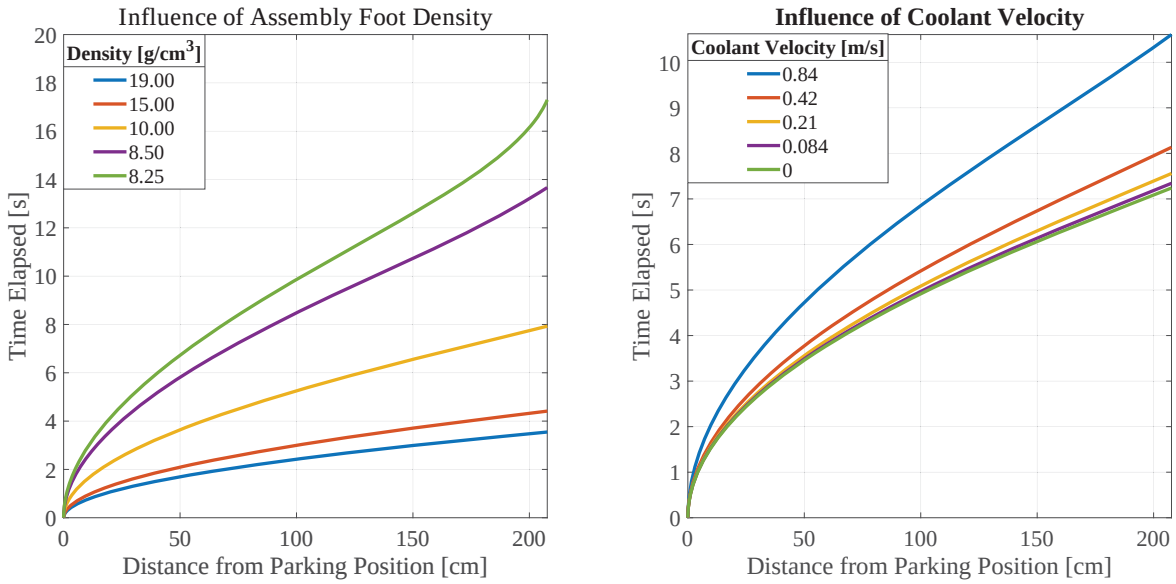


**(a) Sensitivity Study of the Assembly Foot Density (for coolant velocity = 0.84m/s)**

**(b) Sensitivity Study of the Coolant Velocity (for assembly foot density = 9.0g/cm$^3$)**

**Figure 3: Influence of the Foot Density and the Coolant Velocity on Insertion Dynamics**

This comparative study was used to determine a foot density value of 9.0g/cm$^3$ (per assembly equivalent of 16.6kg) that yielded a time of insertion of 10.6s, which was close to the objective of attaining a 10s insertion period. Fig. 4a and 4b depicts the dynamics of the assembly when passively inserted for this optimised configuration of the assembly foot. The scale of the net force shows why the drag force is the limiting force. Any higher drag (coefficient) results in hydrodynamical suspension of the assembly. It is to be noted that buoyancy force increases as the

assembly descends, due to decreasing coolant temperature, while drag force varies depending on instantaneous relative velocity between the coolant and assembly. The net force is positive only for a part of the descent and is negative for the remaining portion. The assembly continues its descent (non-zero positive velocity) on account of its momentum.

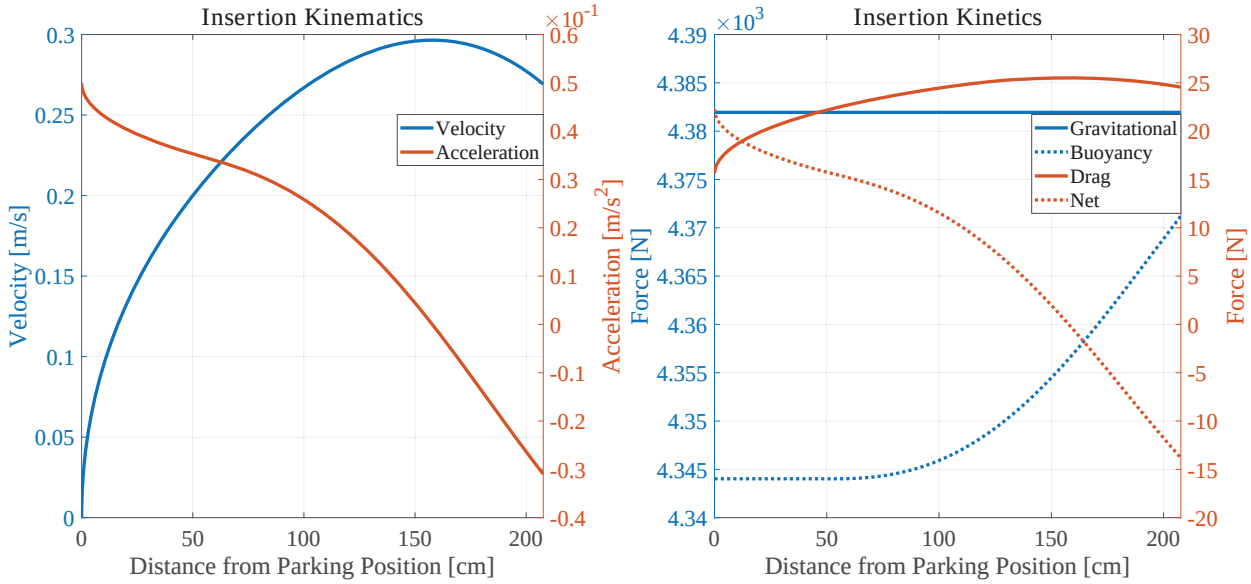


**(a) Velocity and Acceleration of the Optimised Assembly During Gravity-driven Insertion**

**(b) Forces Experienced by the Optimised Assembly During Gravity-driven Insertion**

**Figure 4: Dynamical Parameters During Passive Gravity-driven Insertion in the Channel**

### 3.3. Transient Simulations - Transient Overpower

Since the system, and in turn the insertion model, depends on many parameters, such as the coolant temperature field and flow velocity that vary during a transient, the dynamic analysis of the gravity-driven insertion warrants special interest. In order to assess the system behaviour during transients the model was incorporated in the in-house transient analysis code BELLA. BELLA is a multi-point dynamics code, based on a lumped parameter approach and point-wise description of reactor components, such as the core, the primary system, steam generator, and secondary system [13]. As the code is built in the MATLAB/Simulink environment, a MATLAB function block describing the shutdown model was implemented. This block reads the conditions of the coolant and outputs the inserted reactivity, corresponding to the depth of insertion. BELLA is under development for SEALER-UK and not all transients have yet been benchmarked and would be carried out later in the design procedure. For this study, transient overpower was identified to be critical and was simulated. Anticipated Transient Without SCRAM is a class of transients that occur when the numerous redundant active systems in place fail to shutdown or SCRAM on identifying abnormal operating conditions. The self-actuating device that triggers the insertion is yet to be developed and for this study it was decided to incorporate a Curie-point electromagnetic (CPEM) latch, modeled as a simple switch in BELLA, that demagnetises when the coolant outlet temperature exceeds 770$^o$C, the Curie temperature of pure iron [14].

Overpower transient necessitates special attention because sudden change in reactivity, for instance due to ejection of control rods, is a driving factor for changes in the fuel that instantaneously manifests in power imbalance. This scenario was simulated in BELLA considering that the reactivity insertion due to withdrawal of control rods in SEALER-UK at its critical point is 280pcm ($\approx$ 0.5$ of reactivity). In the dense lead coolant, $B_4C$ control rods have the potential to be ejected in a very short time interval, and 0.5s was the time calculated by a modified version of the program that solves for buoyancy-driven dynamics. Fig. 5a shows the inserted reactivity and the anti-reactivity of the shutdown rods following actuation by the CPEM. For comparison, the figure also shows the anti-reactivity contribution during an accidental SCRAM of the reactor and the contribution after an active actuation with a delay of a nominal 10s (chosen arbitrarily) after transient initiation. The temperature variation of the fuel, clad and coolant outlet are presented in Fig. 5b.

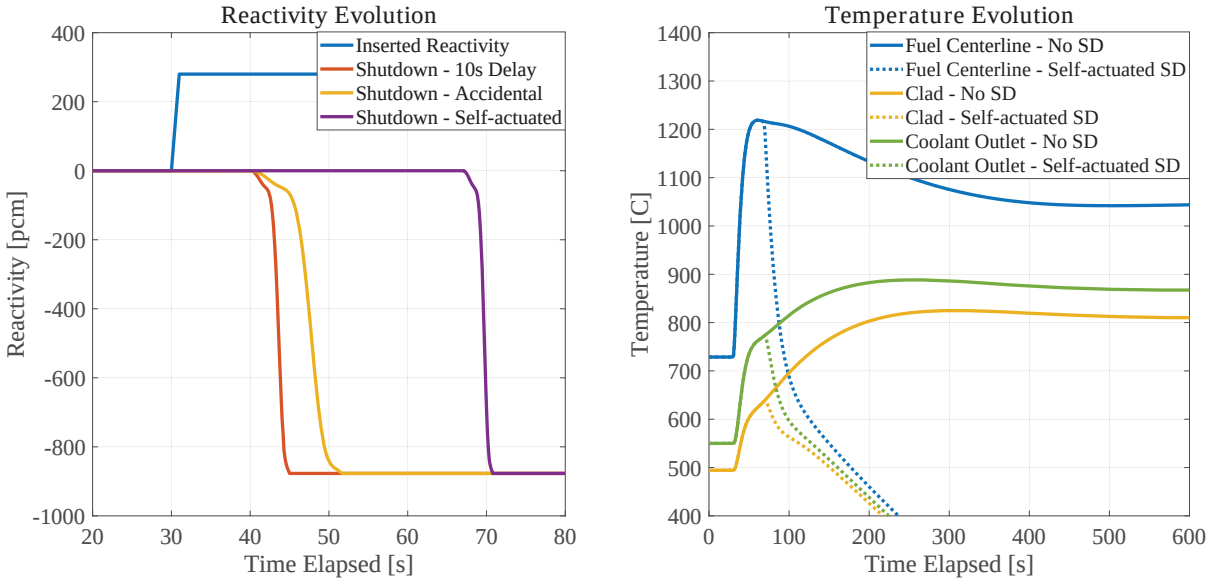


**(a) Evolution of Reactivity from Control Rod Ejection that Eventually Triggers Shutdown**

**(b) Evolution of Temperatures for Protected and Unprotected Transients (SD - Shutdown)**

**Figure 5: Reactivity and Temperature Evolution Following 0.5$ Reactivity Insertion**

## 4. RESULTS AND CONCLUSIONS

The initial temperature spike in the fuel reaches 1225$^o$C, 30s into the transient, which would be smaller if the self-actuation happens at a lower temperature with a suitable CPEM. Nevertheless, this is well below the melting temperature of the nitride fuel, 2250$^o$C. The clad reaches a maximum temperature of 825$^o$C, retaining 165$^o$C margin to melting, 220s into the transient when the reactor is managed only by temperature feedbacks, which also marks that the reactor is passively safe. With eventual shutdown of the reactor, bringing the core sub-critical, BELLA calculates rapidly falling temperature fields. Time of insertion, as calculated from Fig. 5a, during accidental SCRAM was 10.7s, which quite satisfactorily agrees with the 10.6s calculated from the standalone MATLAB program. However, in other cases the gravity-driven system is interestingly inserted in a shorter period. As the CPEM is actuated 37.2s after initiation of the transient when the coolant outlet has reached 770$^o$C, reducing the channel coolant density by 3%, it results in a faster inser-

tion at 3.6s. The reasoning is the same for active actuation with 10s delay, however the insertion is comparatively slower at 5s, because the density reduction is not as high. The delay considered herein, was the same for all assemblies. It is a possibility that the temperature distribution in the upper lead pool is not uniform, demagnetising only one or a few of the CPEM latches, leading to asynchronous actuation. While this is an important aspect, it demands consideration with related systems, such as the Reactor Protection System, which is to be developed for SEALER-UK. This assessment and its impact on shutdown would fall outside the purview of the M.Sc. thesis work, which serves as the basis for this paper, and could be recommended for future exploration.

This investigation showed that an optimally designed shutdown assembly can be passively inserted by gravity in a lead-cooled reactor. While the study focused on a SMR, it is equally applicable in other medium to large sized reactors. The dynamic analysis of control rod ejection accident showed that insertion period was substantially reduced due to the influence of coolant temperatures. This fact can be exploited to perform analysis for other transient scenarios, such as loss of heat sink and more particularly loss of flow, as it was shown that coolant velocity appreciably influences the dynamics. Future work could also include extensive multiphysics investigation of the system using dedicated solvers, and the means to experimentally validate the numerical results.

## REFERENCES

[1] H. A. Abderrahim, P. Baeten, D. D. Bruyn, and R. Fernandez. "MYRRHA – A Multi-purpose Fast Spectrum Research Reactor." *Energy Conversion and Management*, **volume 63**, pp. 4–10 (2012).
[2] J. Wallenius, S. Qvist, I. Mickus, S. Bortot, P. Szakalos, and J. Ejenstam. "Design of SEALER, a Very Small Lead-cooled Reactor for Commercial Power Production in Off-grid Applications." *Nuclear Engineering and Design*, **volume 338**, pp. 23–33 (2018).
[3] J. Ejenstam, M. Halvarsson, J. Weidow, B. Jonsson, and P. Szakalos. "Oxidation Studies of Fe10CrAl-RE Alloys Exposed to Pb at 550°C for 10,000h." *Journal of Nuclear Materials*, **volume 443**, pp. 161–170 (2013).
[4] S. Hayes, J. Thomas, and K. Peddicord. "Material Property Correlations for Uranium Mononitride: I. Physical Properties." *Journal of Nuclear Materials*, **volume 171**, pp. 262–270 (1990).
[5] A. Banerjee, S. Raju, R. Divakar, E. Mohandas, G. Panneerselvam, and M. Antony. "Thermal Property Characterization of a Titanium Modified Austenitic Stainless Steel (Alloy D9)." *Journal of Nuclear Materials*, **volume 347**, pp. 20–30 (2005).
[6] K. Mikityuk. "Heat Transfer to Liquid Metal: Review of Data and Correlations for Tube Bundles." *Nuclear Engineering and Design*, **volume 239**, pp. 680–687 (2009).
[7] J. Leppanen, M. Pusa, T. Viitanen, V. Valtavirta, and T. Kaltiaisenaho. "The Serpent Monte Carlo code: Status, Development and Applications in 2013." *Annals of Nuclear Energy*, **volume 82**, pp. 142–150 (2015).
[8] P. Romano, N. Horelik, B. Herman, A. Nelson, B. Forget, and K. Smith. "OpenMC: A State-of-the-art Monte Carlo Code for Research and Development." *Annals of Nuclear Energy*, **volume 82**, pp. 90–97 (2015).
[9] A. Lech, C. Turner, J. Lei, R. Mohammadi, S. Tolbert, and R. Kaner. "Superhard Rhenium-tungsten Diboride Solid Solutions." *Journal of the American Chemical Society*, **volume 138**, pp. 14398–14408 (2016).
[10] "Live PGM Prices." (2019). URL https://www.metalsdaily.com/live-prices/pgms/.
[11] "Tungsten Price." (2019). URL http://www.metalary.com/tungsten-price/.
[12] J. Wallenius. "Shutdown Rod for Lead-cooled Reactors (Patent WO 2017/105325 A1)." *World Intellectual Property Organization* (2017).
[13] S. Bortot, E. Suvdantsetseg, and J. Wallenius. "BELLA: A Multi-point Dynamics Code for Safety-informed Design of Fast Reactors." *Annals of Nuclear Energy*, **volume 85**, pp. 228–235 (2015).
[14] T. Misao, S. Takashi, A. Takafumi, U. Masato, and K. Shoji. "Demonstration of Control Rod Holding Stability of the Self Actuated Shutdown System in Joyo for Enhancement of Fast Reactor Inherent Safety." *Journal of Nuclear Science and Technology*, **volume 44**, pp. 511–517 (2007).